

Evidence of a Critical Phase Transition in Purely Temporal Dynamics with Long-Delayed Feedback

Marco Faggian,^{1,2} Francesco Ginelli,¹ Francesco Marino,³ and Giovanni Giacomelli⁴

¹*SUPA, Physics Department and Institute for Complex Systems and Mathematical Biology, King's College, University of Aberdeen, Aberdeen AB24 3UE, United Kingdom*

²*Faculty of Information Studies in Novo Mesto, 8000 Novo Mesto, Slovenia*

³*Consiglio Nazionale delle Ricerche, Istituto Nazionale di Ottica, Largo E. Fermi 6, 50125 Firenze, Italy*

⁴*Consiglio Nazionale delle Ricerche, Istituto dei Sistemi Complessi, Via Madonna del Piano 10, 50019 Sesto Fiorentino, Italy*



(Received 25 July 2017; published 26 April 2018)

Experimental evidence of an absorbing phase transition, so far associated with spatiotemporal dynamics, is provided in a purely temporal optical system. A bistable semiconductor laser, with long-delayed optoelectronic feedback and multiplicative noise, shows the peculiar features of a critical phenomenon belonging to the directed percolation universality class. The numerical study of a simple, effective model provides accurate estimates of the transition critical exponents, in agreement with both theory and our experiment. This result pushes forward a hard equivalence of nontrivial stochastic, long-delayed systems with spatiotemporal ones and opens a new avenue for studying out-of-equilibrium universality classes in purely temporal dynamics.

DOI: [10.1103/PhysRevLett.120.173901](https://doi.org/10.1103/PhysRevLett.120.173901)

Introduction.—The concepts of scaling and universality play a prominent role in statistical physics [1]. Starting with early—and pioneering—scaling ideas [2–4] up to renormalization group theory [5,6], they have been successfully applied to develop a comprehensive theory of critical phenomena in equilibrium [7] and, to a large extent, in nonequilibrium systems [8]. Diverging correlation lengths and a scaling of relevant quantities ruled by universal exponents are the signature of such phenomena. In the framework of spatially extended media, universality is uncovered as the system is inspected at increasing length scales and often characterized via spatially resolved measurements of the significant quantities (e.g., correlation functions).

An important question is to what extent the universality classes predicted and observed in spatiotemporal systems can also hold in purely temporal dynamics, without explicit spatial degrees of freedom. In this Letter, we bring the first answer to the above issue by investigating the behavior of a stochastic, long-delayed bistable system.

A delayed feedback sets an infinite-dimensional phase space for the dynamics [9–11]. A special case is the so-called long-delay limit, i.e., when the delay time τ is much longer than any other, internal timescale. Here, a suitable representation [12] permits us to unveil the role of the involved multiple timescales acting as effective spatial variables (for a recent review, see [13]), and a thermodynamic limit is defined as $\tau \rightarrow \infty$. This correspondence has been shown to hold in deterministic systems [14–17] and even put on rigorous grounds close to a Hopf bifurcation [18]. However, in the presence of nontrivial stochastic

processes, only a few numerical studies in simple models have been reported [19,20]. In particular, whether this equivalence is preserved as a critical transition point is approached and correlation lengths diverge has never been tested experimentally.

Here, we address this fundamental question showing that a stochastic, long-delayed bistable laser—where effective spatial degrees of freedom emerge from different, well separated timescales—undergoes a genuine out-of-equilibrium active-to-absorbing critical phase transition, belonging to the directed percolation (DP) universality class in one spatial dimension [21].

Nonequilibrium models related to epidemic spreading [22], gravity-driven percolation of fluids through a porous medium [23], intermittent interface-depinning and synchronization phenomena [24–26], and the transition from laminar to turbulent flows [27–29] are other well-known examples of this universality class, so far mainly associated to genuine spatiotemporal dynamics. Recently, DP and nonequilibrium phase transitions into absorbing states have been investigated in open many-body quantum systems [30–32].

Because of its prominence, DP is commonly regarded as the Ising model of nonequilibrium critical phenomena, but experimental evidence has long been elusive. Only recently, measurements in systems displaying spatiotemporal turbulence [33–35] have provided the first clear evidence of DP critical behavior in one and two spatial dimensions and sparked renewed attention for this ubiquitous nonequilibrium phenomenon.

Experiment.—The experimental setup (Fig. 1) is based on a bistable vertical cavity surface emitting laser (VCSEL)

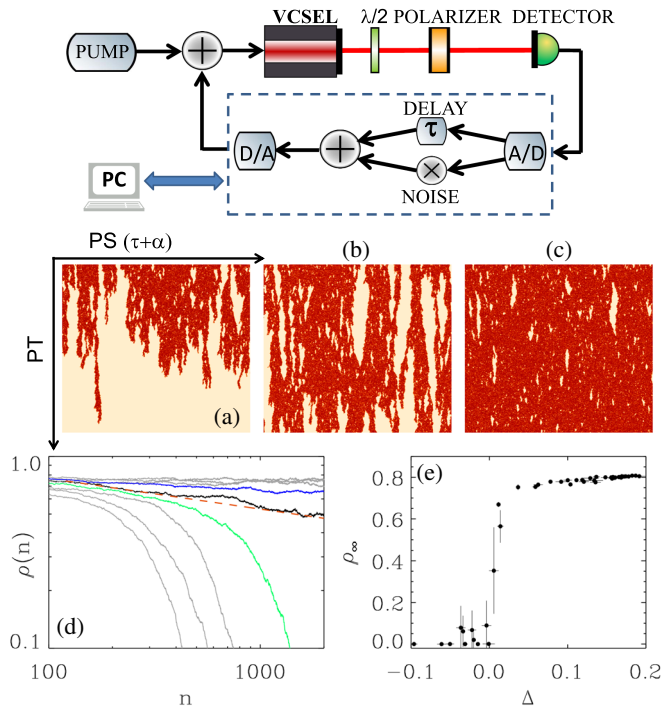


FIG. 1. Experimental setup (top). Center and bottom: experimental laser dynamics with an upper polarization initial condition, for a fixed feedback gain and multiplicative noise amplitude; the delay is $\tau = 190$ ms. (a)–(c) P-ST patterns increasing the laser pump current in the absorbed, critical, and active phase, respectively. Darker colors mark the upper polarized state. The horizontal range is $\tau/10$, and the vertical one spans 2×10^3 delay units. (d) Delay-averaged intensity $\rho(n)$ as a function of PT for different values of the normalized control parameter Δ (see text). The dashed red line is the power law decay for DP scaling theory. (e) Estimated asymptotic intensity ρ_∞ vs Δ .

which, for a particular choice of the pump current, displays the coexistence of two linear polarization states of the emitted optical field [36,37]. The two polarizations are separated by means of a half-wave plate and a polarizing beam splitter, and then, their intensities are monitored by photodetectors. The signal corresponding to the upper state is then acquired, delayed by a time $\tau = 190$ ms and subsequently fed back into the VCSEL through the pump current using a summer circuit. A Gaussian noise, software-generated as a sequence of zero-mean, delta-correlated numbers, is then multiplied to the (nondelayed) main polarization signal and reinjected as well. Because of its multiplicative nature, this noise vanishes on the lower state, while it affects the other polarization inducing spontaneous fluctuations towards the lower state. The delayed feedback is realized sampling the electric signal from the detector with a A/D-D/A board hosted by a PC driven by a real-time Linux OS. The data are treated with a custom software which allow us to choose the initial condition, the gain, and the amount of multiplicative noise.

We begin our experimental test by a visual investigation of evolution of the polarized intensity signal $I(t)$ (in the

following, denoted as intensity). The transformation $t = n\tau + \sigma$ with integer n and real $\sigma \in [0, \tau)$ is used to obtain the corresponding pseudospatiotemporal (P-ST) representation in the plane (σ, n) . The original time series is cut in consecutive segments of length τ , each labeled by the pseudotime (PT) n , and inside each slide σ marks a pseudospace (PS) position in a one-dimensional (1D) space. Because of causality, the information transfer processes are strongly asymmetric in this representation [13], yielding a nonzero drift term with velocity (in P-ST units) $\alpha \ll \tau$. For visualization purposes, we adopt the comoving transformation $t = n'(\tau + \alpha) + \sigma'$ with $\sigma' \in [0, \tau + \alpha)$ [38].

In this representation, the VCSEL intensity is characterized by nucleation, propagation, and annihilation of fronts that, in the absence of multiplicative noise, leads to coarsening [14,17,39]. Notably, the P-ST description allows us to unfold and display the features of the dynamics over a range of peculiar and independent timescales: the width of the fronts separating the upper and lower polarization states (bandwidth limited at a few μ s), the PS correlation length, the delay τ , and the PT correlation length. All of them play a role in our setup. The ratio between τ and the front width corresponds to the aspect ratio, as defined in spatially extended systems [13]. The PS and PT correlation lengths determine the features of the patterns of the active state and are known to scale with the distance from the critical point.

Typical P-ST patterns of the intensity as the pump current is increased and for a fixed multiplicative noise amplitude are shown in Figs. 1(a)–1(c). The system is initialized with a sequence of length τ close to the upper state (with random Gaussian statistics). We observe complicated P-ST dynamics with a relaxation towards either the lower [Fig. 1(a)] or upper [Fig. 1(c)] state. For intermediate values of the pump, the system apparently evolves slowly on longer PT scales.

Such behavior is immediately reminiscent of the active-to-absorbed phase transition, as observed in a large class of reaction diffusion systems with an *absorbing* state (i.e., a state able to trap the dynamics indefinitely). One can readily identify the lower state, preserved by our choice of the multiplicative noise, with such an absorbing state: with other experimental noises carefully minimized, the upper states cannot nucleate spontaneously inside PS homogeneous patches of lower states, which can only be displaced by the invasion of moving fronts. On the contrary, fluctuations can easily nucleate lower state patches inside the upper ones. Moreover, once the laser sets down in the lower state for at least one full delay, its emission has no more chances to jump back to the upper polarized state, being effectively absorbed.

According to the Janssen-Grassberger conjecture [40,41], in the absence of additional symmetries and/or quenched randomness, any spatiotemporal dynamics

displaying such a transition from a fluctuating *active* (i.e., not dynamically frozen) phase into a unique absorbed state is expected to belong to the DP universality class. One should thus expect a critical, power law behavior described by three independent critical exponents, numerically known with high accuracy in 1D [21].

We use as a control parameter the coarsening velocity v in the absence of the multiplicative noise estimated at the beginning and the end of each measurement. While this velocity is strictly related to the pump current, this procedure allows for a more precise determination of the actual working point of the laser (see Supplemental Material, [42]). In particular, we retain only those measurements whose final initial relative difference in the speed is smaller than 3%. As an order parameter, we introduce the delay-averaged intensity $\rho(n) = \langle I(\sigma, n) \rangle_\sigma$, normalized between 0 and 1 and its PT asymptotic value ρ_∞ .

In Fig. 1(d), the PT evolution of $\rho(n)$ is reported for different values of the corresponding coarsening velocity. A clear transition is present from asymptotically nonzero values (the active phase) to an exponential decrease towards zero (absorbing phase). The bold green and blue curves correspond to the patterns shown in Figs. 1(a) and 1(c), respectively. A near-critical curve, displaying a power law decay over more than one decade, is also plotted alongside the known DP asymptotic scaling $\rho(n) \sim n^{-\delta}$ (with $\delta = 0.159464(6)$ [21]), showing a satisfactory agreement between our experiment and DP scaling theory.

We further define the normalized control parameter $\Delta = (v - v_c)/v_c$, where v_c is the empirical critical coarsening velocity, and plot the PT asymptotic value of the order parameter ρ_∞ as a function of Δ . Figure 1(e) clearly shows the signature of a transition between the absorbed ($\Delta < 0$) and active phases ($\Delta > 0$). One would now ideally proceed to measure the scaling of ρ_∞ as the critical point is approached from the active phase, $\rho_\infty \sim \Delta^\beta$ with $\beta = 0.276486(6)$ [21]. Unfortunately, when initialized in the upper state, the system is prone to non-negligible fluctuations in the working point, which prevented us from reaching the large PTs needed for a clear testing of this latter scaling law.

However, we report in Fig. 2 the results of another set of measurements: the so called *single seed* behavior. For every value of the control parameter, the system is prepared in the initial delay cell close to the lower state, except for a set of small intervals—equally spaced along the delay length—which are set in the higher state. This procedure creates an ensemble of 10^2 active seed states which evolve independently as long as their ensuing activity remains separated in PS. The relevant quantities are evaluated as averages over such ensembles. Working point fluctuations are milder for (mainly) lower-state initial conditions, and we achieve a better control over the critical dynamics.

In DP scaling theory, single seed initial conditions may decay into the absorbing state or survive and spread with a time-dependent probability $P(n)$. In the absorbing phase, one expects $P(n) \sim n^{-\delta} \exp(-n/\xi_\parallel)$, where the

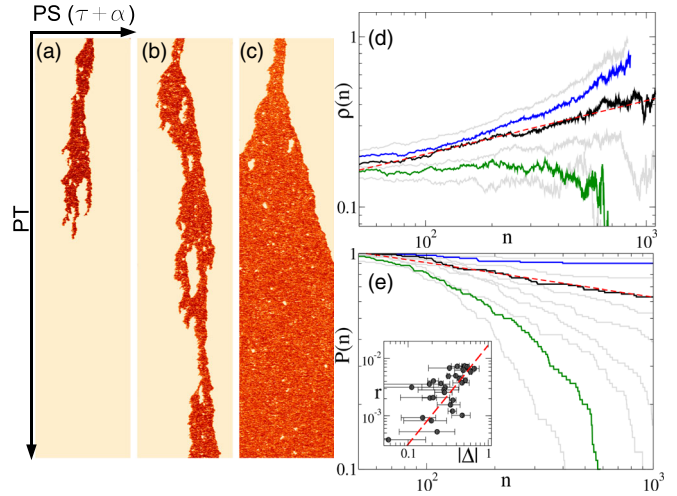


FIG. 2. Experimental laser dynamics with single seed initial conditions (see text). The delay is $\tau = 190$ ms. (a)–(c) P-ST patterns of a single seed in the absorbed, critical, and active phase, respectively. (d) Delay-averaged intensity $\rho(n)$ and (e) survival probability $P(n)$ as a function of PT for different values of the normalized control parameter Δ (see text). Inset: survival probability exponential decay rates $r = 1/\xi_\parallel$ vs $|\Delta|$ in the absorbing phase. The dashed red lines mark the expected DP power law behavior.

temporal correlation length diverges as the critical point is approached: $\xi_\parallel \sim \Delta^{-\nu_\parallel}$ with $\nu_\parallel = \beta/\delta = 1.733847(6)$ being a second independent exponent [21]. Thus, at the critical point, the survival probability decays as a power law $P(n) \sim n^{-\delta}$. A third independent exponent, the so-called initial slip exponent θ , can be finally deduced from the initial growth of activity at the critical point when starting from a single seed (or sparsely active) initial condition $\rho(n) \sim n^\theta$ for $\rho(n) \ll 1$, with $\theta = 0.313686(8)$ [43].

In Figs. 2(a)–2(c), we present three single seed sample patterns showing the onset of a near-critical behavior in Fig. 2(b). We further report in Figs. 2(d) and 2(e) the growth of the delay-averaged signal [Fig. 2(d)] and the survival probability (SP) of a seed [Fig. 2(e)] as a function of PT for different values of Δ . The bold green and blue again denote the subcritical and supercritical behaviors corresponding to the patterns in Figs. 2(a)–2(c); the bold black curve corresponds to the critical case of Fig. 2(b). The dashed lines superimposed in the density and SP plots are the power laws expected for DP at criticality, showing an excellent agreement with the spatiotemporal theory. In the inset of Fig. 2(e), we plot the PT correlation length ξ_\parallel estimated in the subcritical case. In spite of the large errors due to residual working point fluctuations, the results are compatible with the DP power law scaling as depicted by the dashed line.

Model.—In order to corroborate our experimental findings, we introduce a stochastic effective model, derived from the deterministic description of Ref. [14],

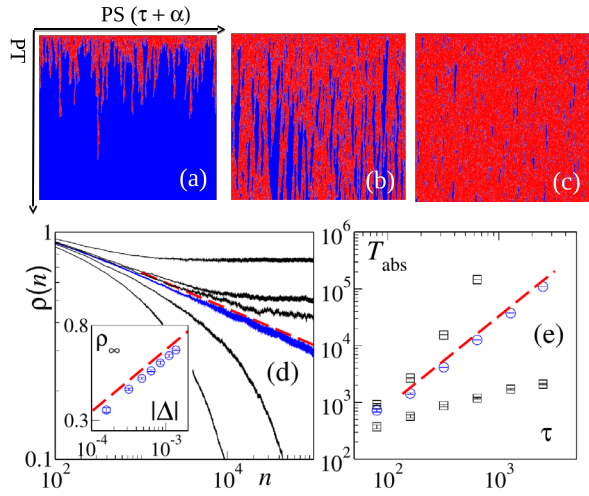


FIG. 3. Simulations of Eq. (1) for fully active initial conditions. Typical P-ST patterns in the (a) absorbed ($a = 0.93$), (b) critical ($a = 0.89455$), and (c) active ($a = 0.86$) phases in a blue ($x_t \approx y_0$) to red ($x_t \approx y_1$) color scale. (d) Delay-averaged intensity $\rho(n)$ for different values of a (from top to bottom: $a = 0.88, 0.885, 0.89, 0.89455, 0.8985, 0.9045$). The delay is $\tau = 2 \times 10^5$; the corrected drift $\alpha = 5.75$. Data have been further averaged over 5 to 50 independent realizations. Inset: scaling of ρ_∞ [estimated by a time-average of $\rho(n)$ over the stationary regime] vs $\Delta = |a - a_c|/a_c$. (e) Mean absorbing time vs τ for different values of a (from top to bottom: $a = 0.891, 0.8947, 0.887$). Data are averaged over 400 realizations. The dashed red lines mark the DP scaling behavior (lower graphs are in log-log scale), while our best fits (not shown) estimate $\delta \approx 0.16(1)$, $\beta \approx 0.28(1)$, $z \approx 1.58(8)$.

$$dx_t = [gx_{t-\tau} + F_a(x_t)]dt + bx_t dW_t \quad (1)$$

where the real variable x_t represents the intensity, dW_t is the increment of a Wiener process, $F_a(x) = -(d/dx)U_a(x) \equiv -x(x-1)(x-a)$ is a force term derived from a bistable quartic potential, and τ is the delay time. The dynamics (1) is controlled by three real parameters: the delayed feedback coupling g , the multiplicative noise amplitude b , and the potential asymmetry a with $a > g > 0$.

The deterministic dynamics ($b = 0$) has two stable fixed points $x_t = y_0 \equiv 0$ and $x_t = y_1 \equiv [(1+a) + \Gamma]/2$, with $\Gamma \equiv \sqrt{(1-a)^2 + 4g}$, separated by the unstable fixed point $x_t = y_u \equiv [(1+a) - \Gamma]/2$. In the absence of delay ($\tau \rightarrow 0$), the deterministic dynamics only consists in a relaxation to equilibria on intrinsic timescales of order $t_0 = (a-g)^{-1}$ and $t_1 = \Gamma^{-1}(1+a+\Gamma)^{-1}$. In the case of a long delay $\tau \gg t_0, t_1$, quasiheteroclinic fronts joining the two stable fixed points can be observed as a transient phenomena. Indeed, the relative stability of the fixed points controlled by system parameters, in particular, by the potential asymmetry a , determines the coarsening dynamics [14].

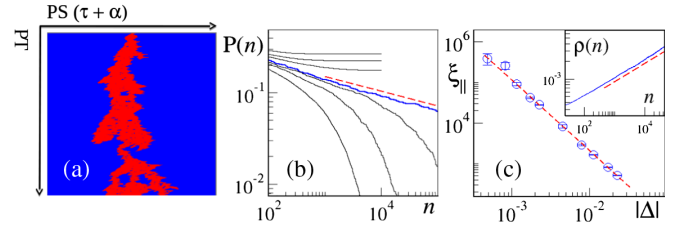


FIG. 4. Single seed simulations. (a) Characteristic P-ST pattern near the critical point $a_c^{ss} \approx 0.89447(2)$. (b) Survival probability $P(n)$ for different values of a (from the top: $a = 0.88, 0.885, 0.89, 0.89447, 0.8955, 0.8985, 0.9045$). (c) Subcritical PT correlation length $\xi_{||}$ [estimated through the fit of $P(n) \sim n^{-\delta} \exp(-n/\xi_{||})$ vs Δ]. Inset: growth of the delay-averaged intensity $\rho(n)$ at the critical point. Data has been averaged over around 10^3 – 10^4 different independent realizations. The dashed red lines mark the DP scaling behavior, while our best fits (not shown) estimate $\delta \approx 0.159(4)$, $\nu_{||} \approx 1.73(2)$, $\theta \approx 0.32(1)$.

In the following, we investigate numerically the full stochastic dynamics for long delays, interpreting Eq. (1) in the Itô sense and adopting a simple Euler-Maruyama integration method with a time stepping $\Delta t = 0.01$ [44]. We fix the noise amplitude $b = 1/\sqrt{7}$ and the delayed feedback coupling $g = 0.22$, using the potential asymmetry a as our main control parameter. We have however verified that analogous results hold using, for instance, g as a control parameter.

We focus on the range $a \in [0.5, 1]$, preparing our system with the initial conditions $x_t = y_1$ for $t \in [0, \tau)$. Our numerical results for the delay-averaged intensity are reported in the P-ST plots of Figs. 3(a)–3(c). For values of the asymmetric parameter a close to 1, the P-ST dynamics quickly drops from the active state to the absorbing one (we consider a state as absorbed when $x_t < y_u$ for one full delay). As a is lowered, the system goes through a phase transition located at $a_c \approx 0.8946(1)$ to reach an active phase. The critical exponents δ and β can be estimated within a 6% accuracy as shown in Fig. 3(d). A third independent exponent can be evaluated by measuring the finite-size scaling of the typical time T_{abs} needed for a finite size system to be absorbed at the critical point. Scaling theory predicts $T_{\text{abs}} \sim \tau^z$ with the dynamical exponent $z = 1.580745(1)$, in very good agreement with our numerical simulations [see Fig. 3(e)].

Single seed simulations, reported in Fig. 4, further confirm the identification of our stochastic dynamics (1) with the DP universality class. The slight deviation between the size asymptotic critical point $a_c^{ss} \approx 0.89447(2)$ and the finite size one reported above for fully active initial conditions is indeed compatible with the expected PS finite size scaling [21] (see Supplemental Material, [42]).

Discussion.—To summarize, we have experimentally shown and numerically confirmed the existence of a DP critical phase transition in the long-delayed dynamics of a bistable system with multiplicative noise. Our system is

purely temporal, and the effective spatial variables involved emerge from the multiple timescales of the dynamics.

While the onset of nonequilibrium critical phenomena in systems with long-delay has been previously put forward in simple model systems [19,20,45], this work represents the first experimental evidence of such behavior. We show that the mapping between long-delayed dynamics and spatio-temporal systems is preserved for stochastic dynamics even as a critical point is approached, so that the former and latter systems may share the same universality class.

Our result opens a new avenue for studying experimentally a number of out-of-equilibrium universality classes—for instance, the Kardar-Parisi-Zhang class [46]—in purely temporal, long-delayed setups. Moreover, the occurrence of critical phenomena and their scalings in higher effective spatial dimensions could be investigated by means of different types of delayed feedbacks with multiple, hierarchically long delays [47].

Furthermore, absorbing phase transitions such as DP may also take place in nonequilibrium many-body quantum systems [30–32], for instance, in interacting gases of Rydberg atoms [32,48]. Moreover, an interesting connection between superradiance in cold atom systems and standard lasing has been recently argued in [49]. In this context, we expect our system—where in appropriate conditions quantum fluctuations due to spontaneous emission could have an impact on the transition—to motivate a larger community interested in phase transition in quantum simulators.

We wish to thank S. Lepri and A. Politi for useful discussions. M. F. and F. G. acknowledge support from EU Marie Curie ITN Grant No. 642563 (COSMOS).

[1] L. P. Kadanoff, *Physica (Amsterdam)* **163A**, 1 (1990).
 [2] B. Widom, *J. Chem. Phys.* **43**, 3892 (1965); **43**, 3898 (1965).
 [3] L. P. Kadanoff, *Physics* **2**, 263 (1966).
 [4] B. L. Halperin and P. C. Hohenberg, *Phys. Rev.* **177**, 952 (1969).
 [5] K. G. Wilson, *Phys. Rev. B* **4**, 3174 (1971); **4**, 3184 (1971).
 [6] K. G. Wilson and M. E. Fisher, *Phys. Rev. Lett.* **28**, 240 (1972).
 [7] J. M. Yeomans, *Statistical Mechanics of Phase Transitions* (Clarendon Press, Oxford, 1991).
 [8] U. C. Tauber, *Annu. Rev. Condens. Matter Phys.* **8**, 185 (2017).
 [9] T. Vogel, *Theorie des Systemes Evolutifs* (Gauthier-Villars, Paris, 1965).
 [10] J. K. Hale, *Theory of Functional Differential Equations* (Springer-Verlag, Berlin, 1977).
 [11] J. D. Farmer, *Physica (Amsterdam)* **4D**, 366 (1982).
 [12] F. T. Arecchi, G. Giacomelli, A. Lapucci, and R. Meucci, *Phys. Rev. A* **45**, R4225 (1992).

[13] S. Yanchuk and G. Giacomelli, *J. Phys. A* **50**, 103001 (2017).
 [14] G. Giacomelli, F. Marino, M. A. Zaks, and S. Yanchuk, *Europhys. Lett.* **99**, 58005 (2012).
 [15] L. Larger, B. Penkovsky, and Y. Maistrenko, *Phys. Rev. Lett.* **111**, 054103 (2013).
 [16] L. Larger, B. Penkovsky, and Y. Maistrenko, *Nat. Commun.* **6**, 7752 (2015).
 [17] J. Javaloyes, T. Ackemann, and A. Hurtado, *Phys. Rev. Lett.* **115**, 203901 (2015).
 [18] G. Giacomelli and A. Politi, *Phys. Rev. Lett.* **76**, 2686 (1996).
 [19] I. G. Szendro and J. M. López, *Phys. Rev. E* **71**, 055203R (2005).
 [20] S. R. Dahmen and H. Hinrichsen, and W. Kinzel, *Phys. Rev. E* **77**, 031106 (2008).
 [21] H. Hinrichsen, *Adv. Phys.* **49**, 815 (2000).
 [22] D. Mollison, *J. R. Statist. Soc. Ser. B* **39**, 283 (1977).
 [23] S. R. Broadbent and J. M. Hammersley, *Proc. Cambridge Philos. Soc.* **53**, 629 (1957).
 [24] J. Rolf, T. Bohr, and M. H. Jensen, *Phys. Rev. E* **57**, R2503 (1998).
 [25] F. Ginelli, V. Ahlers, R. Livi, D. Mukamel, A. Pikovsky, A. Politi, and A. Torcini, *Phys. Rev. E* **68**, 065102(R) (2003).
 [26] F. Ginelli, R. Livi, A. Politi, and A. Torcini, *Phys. Rev. E* **67**, 046217 (2003).
 [27] Y. Pomeau, *Physica (Amsterdam)* **23D**, 3 (1986).
 [28] M. Sipos and N. Goldenfeld, *Phys. Rev. E* **84**, 035304(R) (2011).
 [29] L. Shi, M. Avila, and B. Hof, *Phys. Rev. Lett.* **110**, 204502 (2013).
 [30] M. Marcuzzi, M. Buchhold, S. Diehl, and I. Lesanovsky, *Phys. Rev. Lett.* **116**, 245701 (2016).
 [31] B. Everest, M. Marcuzzi, and I. Lesanovsky, *Phys. Rev. A* **93**, 023409 (2016).
 [32] R. Gutiérrez, C. Simonelli, M. Archimi, F. Castellucci, E. Arimondo, D. Ciampini, M. Marcuzzi, I. Lesanovsky, and O. Morsch, *Phys. Rev. A* **96**, 041602(R) (2017).
 [33] K. A. Takeuchi, M. Kuroda, H. Chaté, and M. Sano, *Phys. Rev. Lett.* **99**, 234503 (2007); *Phys. Rev. E* **80**, 051116 (2009).
 [34] G. Lemoult, L. Shi, K. Avila, S. V. Jalikop, M. Avila, and B. Hof, *Nat. Phys.* **12**, 254 (2016).
 [35] M. Sano and K. Tamai, *Nat. Phys.* **12**, 249 (2016).
 [36] G. Giacomelli, F. Marin, M. Gabrysch, K. H. Gulden, and M. Moser *Opt. Commun.* **146**, 136 (1998).
 [37] M. P. van Exter, M. B. Willemsen, and J. P. Woerdman, *Phys. Rev. A* **58**, 4191 (1998).
 [38] The drift velocity α can be evaluated, for instance, by autocorrelation measurements in the time series.
 [39] G. Giacomelli, F. Marino, M. A. Zaks, and S. Yanchuk, *Phys. Rev. E* **88**, 062920 (2013).
 [40] H. K. Janssen, *Z. Phys. B* **42**, 151 (1981).
 [41] P. Grassberger, *Z. Phys. B* **47**, 365 (1982).
 [42] See Supplemental Material at <http://link.aps.org/supplemental/10.1103/PhysRevLett.120.173901> for more details about experimental and numerical techniques.
 [43] In one spatial dimension, the initial slip exponent θ is related to β and the usual spatial and temporal correlation exponents by the scaling relation $\theta\nu_{\parallel} = \nu_{\perp} - 2\beta$ [21].

- [44] Adopting the Stratonovich interpretation and or different stochastic Integration schemes and time steppings is not expected to change the system universality class.
- [45] S. Lepri, *Phys. Lett. A* **191**, 291 (1994).
- [46] D. Pazò and J.M. López, *Phys. Rev. E* **82**, 056201 (2010).
- [47] S. Yanchuk and G. Giacomelli, *Phys. Rev. Lett.* **112**, 174103 (2014).
- [48] M. Marcuzzi, E. Levi, W. Li, J. P. Garrahan, B. Olmos, and I. Lesanovsky, *New J. Phys.* **17**, 072003 (2015).
- [49] P. Kirton and J. Keeling, *New J. Phys.* **20**, 015009 (2018).